

Article

Substituent Effects of Adamantyl Group on Amido Ligand in Syndiospecific Polymerization of Propylene with *Ansa*-Dimethylsilylene(Fluorenyl)(Amido) Zirconium Complex

Yanjie Sun ¹, Shuhui Li ¹, Takeshi Shiono ^{2,*}  and Zhengguo Cai ^{1,*} 

¹ State Key Laboratory for Modification of Chemical Fibers and Polymer Materials, College of Material Science and Engineering, Donghua University, Shanghai 201620, China; syj-178@163.com (Y.S.); 15000855167@163.com (S.L.)

² Graduate School of Engineering, Hiroshima University, Higashi-Hiroshima 739-8527, Japan

* Correspondence: tshiono@hiroshima-u.ac.jp (T.S.); caizg@dhu.edu.cn (Z.C.); Tel.: +81-82-424-7730 (T.S.); Tel./Fax: +86-21-6779-2453 (Z.C.)

Received: 21 October 2017; Accepted: 16 November 2017; Published: 21 November 2017

Abstract: A series of new fluorenylamido-ligated zirconium complexes bearing an electron-donating adamantyl group on the amido ligand were synthesized and characterized by elemental analysis, ¹H NMR, and single crystal X-ray analysis. The coordination mode of the fluorenyl ligand to the zirconium metal was η^3 manner, and all the complexes were C_s -symmetric in solution. The complexes showed moderate activity (1.0×10^5 g-polymer mol-Zr⁻¹·h⁻¹), even at a low Al/Zr ratio of 50. The increase of propylene pressure improved the activity by one order of magnitude (up to 1.0×10^6 g-polymer mol-Ti⁻¹·h⁻¹). All catalyst systems gave syndiotactic polypropylene, where the complex containing the 3,6-di-*t*-butyl fluorenyl ligand was more effective for the enhancement of the syndiospecificity. The increase of propylene pressure also improved the syndiospecificity with the syndiotactic pentad of 0.96 and the melting point of 159 °C.

Keywords: constrained geometry catalysts; zirconium complex; adamantyl substituent; propylene polymerization; syndiospecificity

1. Introduction

Developments of single-site catalysts based on group-4 metallocenes demonstrated a well-defined mechanism for the relationship between the symmetry of the complex and the stereospecificity, in which a little change of the ligand dramatically influenced the polymerization performances, such as the activity, stereospecificity, and molecular weight [1–3]. Ewen et al. first reported the preparation of syndiotactic polypropylene (*syn*-PP) by using C_s -symmetric metallocene in 1988 [4]. Since this report, much effort has been made towards achieving the synthesis of *syn*-PP with single-site catalysts, including doubly bridged metallocenes [5], constrained geometry catalysts (CGCs) [6], and nonmetallocene catalysts [7–12]. Among these catalysts, group-4 CGCs have attracted much attention for their capabilities of improving copolymerization ability [13–22], stereospecificity [23–27], and living polymerization characteristics [28,29]. Many attempts have been made to improve the catalytic performance of CGC catalysts by changing the electronic and steric properties of the ligand.

Razavi et al. reported that the introduction of *t*-butyl substituent on the fluorenyl ligand of [Me₂Si(*t*-Bu-N)(di-*t*-Bu-Flu)ZrCl₂] (**Zr(a-c)**, Figure 1) improved both the activity and *syn*-specificity with *syn*-pentad (rrrr) of 0.87 [23,24]. Miller et al. demonstrated that sterically expanded zirconium complex (**Zr(d)**, Figure 1) combined with methylaluminoxane (MAO) was strikingly active to give *syn*-PP with unsurpassed *syn*-specificity (rrrr > 0.99) and melting temperature (T_m up to 165 °C) [25].

The results indicated that alkyl substituents on the fluorenyl ligand of zirconium complexes play an important role in catalytic activity and *syn*-specificity. However, the electronic effect of the amido ligand was not investigated.

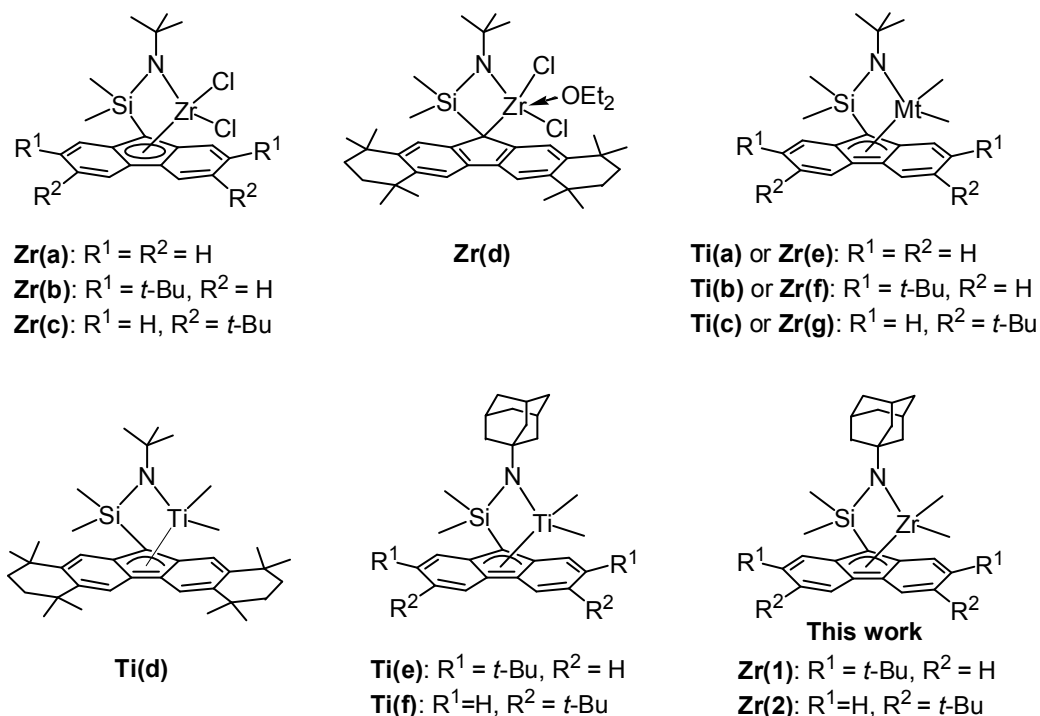


Figure 1. Structures of *ansa*-(fluorenyl)(amido)-ligated complexes.

We previously synthesized the corresponding dimethyltitanium complexes (**Ti(a–c)**, Figure 1) and found that the introduction of *t*-butyl group on the 3,6-position of the fluorenyl ligand improved both the activity and *syn*-specificity in the living polymerization of propylene [30]. However, sterically expanded titanium complex (**Ti(d)**, Figure 1) showed low *syn*-specificity, which differed from that of the corresponding zirconium complex **Zr(d)** [31]. On the other hand, dimethylzirconium complexes $[\text{Me}_2\text{Si}(t\text{-Bu-N})(\text{di-}t\text{-Bu-Flu})\text{ZrMe}_2]$ (**Zr(e–g)**, Figure 1) showed very low activity for propylene polymerization [32]. Recently, we reported that the introduction of an electron-donating adamantyl substituent on the amido ligand of dimethyltitanium complexes (**Ti(e–f)**, Figure 1) exhibited remarkably high activity with an Al/Ti ratio of 20 without changing *syn*-specificity or livingness [33,34]. In this paper, we synthesized dimethylzirconium complexes (**Zr(1)** and **Zr(2)**, Figure 1) by using the same ligand to investigate the substitute effects of the adamantyl group on the amido ligand of fluorenylamido-ligated zirconium complexes in propylene polymerization.

2. Experimental Section

2.1. Materials

All operations were carried out under N_2 by using standard Schlenk techniques, and all solvents were purified by a PS-MD-5 solvent purification system (Innovative Technology (China) Ltd., Hong Kong, China). A research grade propylene was purified by being passed through a dehydration column of ZHD-20 and a deoxidation column of ZHD-20A before use. Modified methylaluminoxane (MMAO) was donated by Tosoh-Finechem Co. (Shunan, Japan). The ligands and zirconium complexes were prepared according to the procedure reported in the literature [32,33].

2.2. Synthesis of Complexes

2.2.1. Synthesis of [(1-Adamantyl)NSiMe₂(2,7-di-*t*-BuFlu)]ZrMe₂ (**Zr(1)**)

MeLi (1.6 M in ether 10.5 mL, 16.8 mmol) was added dropwise at $-20\text{ }^{\circ}\text{C}$ to a solution of ligand (2,7-di-*t*-BuFlu)SiMe₂(1-Adamantyl) (1.94 g, 4.0 mmol) in 60 mL of diethylether. The resultant orange solution was stirred at room temperature for 4 h. To a solution of ZrCl₄ (0.93 g, 4.0 mmol) in 30 mL pentane, the diethylether solution of the lithium salt was added, which gave a yellow suspension. After stirring for 12 h, the solvent was removed and the residue was extracted with hexane. Then the hexane solution was concentrated and cooled at $-30\text{ }^{\circ}\text{C}$ to yield **Zr(1)** as yellow crystals (0.72 g, 1.24 mmol, 31% yield).

¹H NMR (CDCl₃) (Figure S1): δ = 8.00 (d, 2H, Flu); 7.73 (s, 2H, Flu); 7.45 (dd, 2H, Flu); 2.07 (s, 3H, Ad); 1.80(d, 6H, Ad); 1.64 (d, 6H, Ad); 1.41 (s, 18H, *t*-Bu-Flu); 0.84 (s, 6H, SiCH₃); -0.11 (s, 6H, ZrCH₃). ¹³C NMR (CDCl₃) (Figure S2): 150.8 (Flu); 136.0 (Flu); 122.9 (Flu); 122.4 (Flu); 122.1 (Flu); 120.5 (Flu); 56.1 (Flu); 48.0 (Zr-(CH₃)₂); 39.6 (Ad); 36.5 (Ad); 35.4 (Flu-(C(CH₃)₃)₂); 31.8 (Ad); 31.5 (Flu-(C(CH₃)₃)₂); 30.3 (Ad); 7.2 (Si-(CH₃)₂). Elemental analysis for C₃₅H₅₁NSiZr (calc/found, %): C, 69.47/69.26; H, 8.50/8.41; N, 2.31/2.26.

2.2.2. Synthesis of [(1-Adamantyl)NSiMe₂(3,6-di-*t*-BuFlu)]ZrMe₂ (**Zr(2)**)

Complex **Zr(2)** was synthesized in a method similar to that for **Zr(1)**, and yellow crystals were obtained in 33% yield.

¹H NMR (CDCl₃) (Figure S3): δ = 8.06 (s, 2H, Flu); 7.70 (d, 2H, Flu); 7.46 (dd, 2H, Flu); 2.06 (s, 3H, Ad); 1.82 (d, 6H, Ad); 1.64 (d, 6H, Ad); 1.46 (s, 18H, *t*-Bu-Flu); 0.82 (s, 6H, SiCH₃); -1.05 (s, 6H, ZrCH₃). ¹³C NMR (CDCl₃) (Figure S4): 147.1 (Flu); 134.0 (Flu); 127.2 (Flu); 124.7 (Flu); 124.4 (Flu); 118.3 (Flu); 56.1 (Flu); 48.1 (Zr-(CH₃)₂); 39.6 (Ad); 36.5 (Ad); 35.1 (Flu-(C(CH₃)₃)₂); 32.0 (Ad); 31.9 (Flu-(C(CH₃)₃)₂); 30.3(Ad); 7.0 (Si-(CH₃)₂). Elemental analysis for C₃₅H₅₁NSiZr (calc/found, %): C, 69.47/69.38; H, 8.50/8.46; N, 2.31/2.29.

2.3. Polymerization Procedure

Atmospheric polymerization of propylene was performed in a 100-mL glass reactor equipped with a magnetic stirrer and carried out according to the semi-batch method. At first, the reactor was charged with prescribed amounts of MMAO/2,6-di-*tert*-butyl-4-methyl phenol (BHT) or dired MMAO (dMMAO) and solvent (heptane). After the solution of the cocatalyst was saturated with gaseous propylene under atmospheric pressure, polymerization was started by the addition of 1 mL solution of the zirconium complex in heptane, and the consumption rate of propylene was monitored by a mass flow meter.

High pressure polymerization of propylene was performed in a 200-mL Quick-Open Micro Autoclaves/Pressure Vessel purchased from Anhui Kemi Machinery Technology Co., Ltd. (Hefei, China) Before polymerization, the reactor was cleaned and evacuated at $110\text{ }^{\circ}\text{C}$ for 1 h. Certain amounts of the MMAO/BHT, heptane were added into the reactor under a nitrogen atmosphere, and the mixture was stirred continuously. When the temperature was established, the catalyst solution of heptane was added into the reactor. The reactor was then pressurized with propylene. The polymerization was conducted for a certain time, and terminated with acidic alcohol. The polymers obtained were washed by alcohol to remove MMAO and ligand residue, and dried under vacuum at $80\text{ }^{\circ}\text{C}$ for 6 h until a constant weight was reached.

2.4. Analytical Procedure

The single crystals were mounted under a nitrogen atmosphere at a low temperature, and data collection was made on a Bruker APEX2 diffractometer (Bruker, Karlsruhe, Germany) using graphite monochromated with Mo Ka radiation ($=0.71073\text{ \AA}$). The SMART program package (University of Göttingen, Göttingen, Germany) was used to determine the unit cell parameters. The absorption

correction was applied using the SADABS program (University of Göttingen, Göttingen, Germany) [35]. All structures were solved by direct methods and refined on F^2 by full-matrix least-squares techniques with anisotropic thermal parameters for non-hydrogen atoms. Hydrogen atoms were placed at calculated positions and were included in the structure calculation. Calculations were carried out using the SHELXS-97, SHELXL-2014, or Olex2 program (Bruker AXS Inc., Madison, WI, USA) [36–41]. Crystallographic data are summarized in Table 1.

Table 1. Crystallographic data and parameters for **Zr(1)** and **Zr(2)**.

Complex	Zr(1)	Zr(2)
Formula	C ₃₅ H ₅₁ NSiZr	C ₃₅ H ₅₁ NSiZr
Formula weight	605.07	605.07
Crystal system	Triclinic	Monoclinic
Space group	$P\bar{1}$	$P1\ 2_1/c1$
<i>a</i> (Å)	10.5309(10)	12.673(3)
<i>b</i> (Å)	11.6688(11)	19.886(4)
<i>c</i> (Å)	14.6617(14)	14.198(3)
<i>B</i> (deg)	75.818(2)	111.899(4)
<i>V</i> (Å ³)	1584.3(3)	3320.0(12)
<i>Z</i>	2	4
<i>F</i> (000)	644	1288
D _{calcd.} (g·cm ^{−3})	1268	1211
μ (mm ^{−1})	0.408	0.390
Theta range for data collection	1.924 to 30.715°	1.842 to 25.499°
Reflections collected	16,281	23,033
Independent reflections	9719 [<i>R</i> (int) = 0.2619]	6155 [<i>R</i> (int) = 0.0635]
Final <i>R</i> indices [<i>I</i> > 2 σ (<i>I</i>)]	<i>R</i> 1 = 0.0387, <i>wR</i> 2 = 0.0905	<i>R</i> 1 = 0.0546, <i>wR</i> 2 = 0.1417

Molecular weights and molecular weight distributions of polymers were measured by a polymer laboratory PL GPC-220 chromatograph (Agilen, Santa Clara, CA, USA) equipped with one PL1110-1120 column and two PL MIXED-B 7.5 × 300 mm columns at 150 °C using 1,2,4-trichlorobenzene as a solvent. The parameters for universal calibration were $K = 7.36 \times 10^{-5}$, $\alpha = 0.75$ for polystyrene standard and $K = 1.03 \times 10^{-4}$, $\alpha = 0.78$ for PP samples. Differential scanning calorimeter (DSC) analyses were performed on a TA Q2000 instrument (Waters, New Castle, DE, USA) and the DSC curves of the samples were recorded under a nitrogen atmosphere at a heating rate of 10 °C/min from 40 to 200 °C. The ¹H NMR spectra of complexes were recorded and the ¹³C NMR spectra of PPs were measured on a Bruker Ascend™ 600 spectrometer (Bruker, Karlsruhe, Germany). The chemical shifts of the ¹H NMR spectra were referenced to the residual proton resonance of chloroform-*d* (δ : 7.26), and the ¹³C NMR spectra of PPs were recorded at 110 °C and referenced to the resonance of 1,1,2,2-tetrachloroethane-*d*₂ (δ : 74.47).

3. Results and Discussion

3.1. Molecular Structure of Complexes

The zirconium complexes were synthesized by a one-pot reaction of the corresponding ligand with 4 equivalent of methyl lithium and 1 equiv of ZrCl₄. ¹H NMR spectrum of the methyl groups bonded to Zr and Si atoms in both zirconium complexes indicated that the complexes exhibited a C_s-symmetric nature in solution, respectively. The molecular structures of **Zr(1)** and **Zr(2)** were characterized by single crystal X-ray analysis. The structures are shown in Figure 2, and the selected bond lengths and angles of complexes are shown in Table 2. The lengths between the zirconium metal and five-member carbons of fluorenyl ligand in **Zr(1)** and **Zr(2)** are very close to those previously

reported for *t*-butyl amido complex (**Zr(f)**), in which the fluorenyl ligand was coordinated to the zirconium in an η^3 manner. We applied Tolman cone angles of the amino ligand (θ value in Table 1) to evaluate the steric effect of the amido ligand [42]. The θ values of **Zr(1)** and **Zr(2)** were 71.06 and 68.80°, respectively, which were close to that of the previously reported **Zr(f)** (70.12°). These results indicated that *t*-butyl and 1-admantyl groups possess a similar steric environment around the cationic zirconium metal, thus maintaining the hapticity of the fluorenyl ligand. We therefore can investigate the true electronic effect of the adamantyl substituent on the amido ligand with these fluorenylamido-ligated zirconium complexes for propylene polymerization.

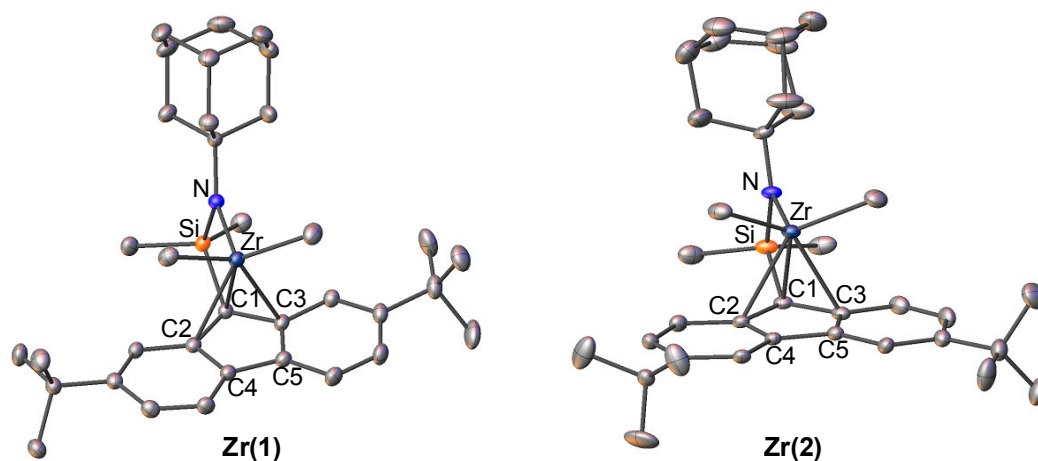


Figure 2. Structure of fluorenylamidotitanium complexes **Zr(1)** and **Zr(2)**. Hydrogen atoms are omitted for clarity. Atoms are drawn at the 40% probability level.

Table 2. Selected bond lengths (Å) and bond angles (degrees) for related complexes.

Parameters	Zr(1)	Zr(2)	Zr(f)
Zr(1)-C(1)	2.3960(17)	2.402(5)	2.385(3)
Zr(1)-C(2)	2.5443(17)	2.535(5)	2.563(3)
Zr(1)-C(3)	2.4948(17)	2.524(5)	2.486(3)
Zr(1)-C(4)	2.6871(17)	2.664(4)	2.702(3)
Zr(1)-C(5)	2.6706(17)	2.655(4)	2.667(3)
Zr(1)-N(1)	2.0536(15)	2.061(4)	2.058(3)
Zr(1)-Si(1)	2.9867(6)	3.005(16)	2.981(3)
$\theta^a = 2/3 (\theta_1 + \theta_2 + \theta_3)$	71.06	68.80	70.12

^a Tolman cone angle of amido groups.

3.2. Propylene Polymerization

Propylene polymerizations were performed by **Zr(1)** and **Zr(2)** activated with trialkylaluminum-free dried MMAO (dMMAO) under atmospheric pressure of propylene in heptane at 0 and 20 °C, and the results are summarized in Table 3. For comparison, the same polymerization conditions as those previously reported for propylene polymerization using **Zr(f)** and **Zr(g)** were employed [32]. The complexes **Zr(f)** and **Zr(g)** conducted propylene polymerization at 20 °C, although they did not show any activity at 0 °C. On the other hand, **Zr(1)** and **Zr(2)** carried out propylene polymerization with moderate activity of $\sim 1.2 \times 10^5$ g-polymer mol-Zr⁻¹·h⁻¹ to produce low molecular weight PP, even at 0 °C. The activities of **Zr(1)** and **Zr(2)** were higher than those of **Zr(f)** and **Zr(g)** at 20 °C. The results testified that the electronic effect of the adamantyl group on the amido ligand plays an important role in this catalyst system rather than having a steric effect, since **Zr(1)**, **Zr(2)**, and **Zr(g)** possess a similar steric environment around the amido ligand. The high

performance of **Zr(1)** and **Zr(2)** can be ascribed to the decreased electrophilicity of the zirconium cation caused by the electron-donating adamantyl group [43], which enhances the separation of the counter anion.

Table 3. Results of propylene polymerization with zirconium complexes ^a.

Entry	cat.	Cocatalyst	Al/Zr	P (atm)	Temp (°C)	Time (min)	Yield (g)	Activity ^d ($\times 10^3$)	M_n ^e ($\times 10^3$)	MWD ^e	T_m ^f (°C)
1	Zr(1)	dMMAO	400	1	0	30	1.29	129	4.4	1.51	139
2	Zr(2)	dMMAO	400	1	0	30	1.17	117	3.8	1.42	155
3	Zr(1)	dMMAO	400	1	20	30	3.23	323	2.5	1.67	132
4	Zr(2)	dMMAO	400	1	20	30	3.56	356	3.1	1.53	148
5 ^b	Zr(f)	dMMAO	400	1	0	30	0	0	-	-	-
6 ^b	Zr(g)	dMMAO	400	1	0	30	0	0	-	-	-
7 ^b	Zr(f)	dMMAO	400	1	20	30	1.77	177	1.17	1.43	125
8 ^b	Zr(g)	dMMAO	400	1	20	30	1.39	139	1.39	1.67	145
9	Zr(1)	MMAO/BHT	400	1	0	30	2.12	212	5.2	1.55	139
10	Zr(1)	MMAO/BHT	200	1	0	30	1.52	152	4.8	1.43	138
11	Zr(1)	MMAO/BHT	100	1	0	30	0.99	99	4.1	1.5	138
12	Zr(1)	MMAO/BHT	50	1	0	30	0.95	95	3.8	1.47	138
13 ^c	Zr(1)	MMAO/BHT	400	8	0	8	1.2	900	7.4	1.81	142
14 ^c	Zr(2)	MMAO/BHT	400	8	0	8	1.35	1012	2.8	2.32	159

^a Polymerization conditions: Heptane = 30 mL, Zr = 20 μ mol, propylene = 1 atm; ^b Data taken from Reference [32];

^c Zr = 10 μ mol; ^d Activity in g of PP/(mol of Ti.h); ^e Number-average molecular weight and molecular weight distribution determined by gel-permeation chromatography GPC using universal calibration; ^f Melting points determined by DSC.

The use of the modification of trialkylaluminum in MMAO with 2,6-di-*tert*-butyl-4-methyl phenol (BHT) as the cocatalyst [44,45] resulted in levels of activity approximately twice as high (up to 2.1×10^5 g-polymer mol-Zr⁻¹·h⁻¹). The same phenomenon was also observed in propylene polymerization with fluorenylamido-ligated dimethyl titanium catalysts (**Ti(e-f)**), where the presence of *i*Bu₂Al(OC₆H₂*t*Bu₂Me) derived from the reaction of *i*Bu₃Al and BHT promoted the efficient separation of the active ion pair to improve the activity [33].

The high cost of single-site catalysts, owing to the requirement of a very high Al/metal ratio to achieve high activity, is a serious limitation for industrial applications. The effect of the Al/Zr ratio in these catalysts was thus investigated (entries 9–12). Although the activity decreased according to the decrease of the Al/Zr ratio from 400 to 100, complex **Zr(1)** still showed moderate activity of 1.0×10^5 g-polymer mol-Zr⁻¹·h⁻¹ even with an Al/Zr ratio of 50 (entry 12), the value of which was comparable to those of **Zr(1)** and **Zr(2)** activated by dMMAO with Al/Ti = 400.

The increase of propylene pressure from 1.0 to 8.0 atm resulted in the increase of the activity by one order of magnitude (up to $\sim 1.0 \times 10^6$ g-polymer mol-Ti⁻¹ h⁻¹, entries 13 and 14). We previously reported that the propagation rate of propylene polymerization with **Ti(a-c)**-dMMAO at 0 °C was increased linearly against the propylene pressure [46].

The melting temperatures of the PPs obtained are also shown in Table 2. All of the catalyst systems gave crystalline polymers with high T_m values. The PP obtained with **Zr(2)** showed a higher T_m value than that obtained with **Zr(1)** in the same polymerization conditions, and the T_m value slightly increased with the increase of the propylene pressure in each catalyst system. A higher T_m value should be ascribed to the higher *syn*-tacticity of PP.

The steric pentad distributions calculated by the ¹³C NMR spectra (Figures S5 and S6) of the methyl region of PPs are shown in Table 4. The results indicated that the PPs obtained were syndiotactic with high rrrr value, and the PP obtained by **Zr(2)** showed a higher rrrr value of 0.96. The *syn*-specific polymerization was conducted via an enantiomorphic site-controlled mechanism with a C_s-symmetric catalyst. In this system, two types of stereodefects are present: one is rmrr arising from the chain migration without monomer insertion, and the other is rmmr arising from the monomer mis-insertion [4]. Both rmrr and rmmr values were decreased in the following order: **Zr(1)** (0.026) > **Zr(2)** (0.003) and **Zr(1)** (0.021) > **Zr(2)** (0.007). These results indicated that the *t*-butyl groups at the 3,6-position of the fluorenyl ligand effectively improve the chain migration and enantioselectivity of the propylene monomer. This result is in agreement with that of propylene polymerization with

Ti(b-c)-dMMAO, where the 3,6-position was more effective than the 2,7-position in improving *syn*-specificity [30].

Table 4. Steric pentad distributions for samples in Table 3 (entries 13 and 14) ^a.

Catalyst	Stereosequence Distribution ^a								
	mmmm	mmm r	rmm r	mm rr	mm r m + r m rr	r m r m	rrrr	mrrr	mrrm
Zr(1)	0.00	0.00	0.021	0.043	0.026	0.021	0.820	0.069	0.00
Zr(2)	0.00	0.00	0.007	0.014	0.003	0.00	0.958	0.018	0.00

^a Determined by ¹³C NMR spectroscopy.

4. Conclusions

The substituent effects of an electron-donating adamantyl group on the amido ligand of fluorenylamido-ligated zirconium catalysts were investigated. Complexes Zr(1) and Zr(2) showed moderate activity of $\sim 1.0 \times 10^5$ g-polymer mol-Zr⁻¹·h⁻¹ with a low Al/Ti ratio of 50. Complex Zr(2) containing 3,6-di-*t*-butyl fluorenyl ligand and the increase of propylene pressure were effective for the improvement of polymerization activity (up to 1.0×10^6 g-polymer mol-Zr⁻¹·h⁻¹) and *syn*-specificity to produce a highly *syn*-tactic PP with an rrrr value of 0.96 and a melting point of 159 °C. These results are in good agreement with the substituent effects of the adamantyl group on the amido ligand of the fluorenylamido-ligated titanium complex.

Supplementary Materials: The following are available online at www.mdpi.com/2073-4360/9/11/632/s1, Figure S1: ¹H NMR spectrum of complex Zr(1), Figure S2: ¹³C NMR spectrum of complex Zr(1), Figure S3: ¹H NMR spectrum of complex Zr(2), Figure S4: ¹³C NMR spectrum of complex Zr(2), Figure S5: ¹³C HMR spectrum of the methyl region of polypropylene obtained with Zr(1) (entry 13, Table 3), Figure S6: ¹³C HMR spectrum of the methyl region of polypropylene obtained with Zr(2) (entry 14, Table 3).

Acknowledgments: This work was supported by National Natural Science Foundation of China (Grant No. 21174026), the program for New Century Excellent Talents in University, the Program for Professor of Special Appointment (Eastern Scholar) at Shanghai Institutions of Higher Learning, “Shu Guang” project supported by Shanghai Municipal Education Commission and Shanghai Education Development Foundation, and the Fundamental Research Funds for the Central Universities. The authors thank Tosoh-Finechem Co. for generously donating the MMAO.

Author Contributions: All authors tried their best to contribute effectively to perform and analyze this experimental work. They all participated in the writing of the present manuscript. Yanjie Sun performed the experimental work. Shuhui Li participated in the analysis of structural data. The setup of the experimental protocol as well as the interpretation of the obtained results were performed under the supervision of Zhengguo Cai and Takeshi Shiono.

Conflicts of Interest: The authors declare no conflict of interest.

References

- Brintzinger, H.H.; Fischer, D.; Mülhaupt, R.; Rieger, B.; Waymouth, R.M. Stereospecific olefin polymerization with chiral metallocene catalysts. *Angew. Chem. Int. Ed.* **1995**, *34*, 1143–1170. [[CrossRef](#)]
- Resconi, L.; Cavallo, L.; Fait, A.; Piemontesi, F. Selectivity in propene polymerization with metallocene catalysts. *Chem. Rev.* **2000**, *100*, 1253–1346. [[CrossRef](#)] [[PubMed](#)]
- Kaminsky, W. Olefin polymerization catalyzed by metallocenes. *Adv. Catal.* **2001**, *46*, 89–159.
- Ewen, J.A.; Jones, R.L.; Razavi, A.; Ferrara, J.D. Syndiospecific propylene polymerizations with group 4 metallocenes. *J. Am. Chem. Soc.* **1988**, *110*, 6255–6256. [[CrossRef](#)] [[PubMed](#)]
- Veghini, D.; Henling, L.M.; Burkhardt, T.J.; Bercaw, J.E. Mechanisms of stereocontrol for doubly silylene-bridged C_s- and C₁-symmetric zirconocene catalysts for propylene polymerization. Synthesis and molecular structure of Li₂[(1,2-Me₂Si)₂(C₅H₂₋₄-(1*R*,2*S*,5*R*-menthyl))₂]{C₅H-3,5-(CHMe₂)₂}}·3THF and [(1,2-Me₂Si)₂{η⁵-C₅H₂₋₄-(1*R*,2*S*,5*R*-menthyl)}₂]{η⁵-C₅H-3,5-(CHMe₂)₂}}ZrCl₂. *J. Am. Chem. Soc.* **1999**, *121*, 564–573.

6. McKnight, A.L.; Waymouth, R.M. Group 4 *ansa*-cyclopentadienyl-amido catalysts for olefin polymerization. *Chem. Rev.* **1998**, *98*, 2587–2598. [[CrossRef](#)] [[PubMed](#)]
7. Ittel, S.D.; Johnson, L.K.; Brookhart, M. Late-metal catalysts for ethylene homo- and copolymerization. *Chem. Rev.* **2000**, *100*, 1169–1203. [[CrossRef](#)] [[PubMed](#)]
8. Gibson, V.C.; Spitzmesser, S.K. Advances in non-metallocene olefin polymerization catalysis. *Chem. Rev.* **2003**, *103*, 283–315. [[CrossRef](#)] [[PubMed](#)]
9. Makio, H.; Terao, H.; Iwashita, A.; Fujita, T. FI catalysts for olefin polymerization—A comprehensive treatment. *Chem. Rev.* **2011**, *111*, 2363–2449. [[CrossRef](#)] [[PubMed](#)]
10. Mu, H.; Pan, L.; Song, D.; Li, Y. Neutral nickel catalysts for olefin homo- and copolymerization: Relationships between catalyst structures and catalytic properties. *Chem. Rev.* **2015**, *115*, 12091–12137. [[CrossRef](#)] [[PubMed](#)]
11. Coates, G.W. Precise control of polyolefin stereochemistry using single-site metal catalysts. *Chem. Rev.* **2000**, *100*, 1223–1252. [[CrossRef](#)] [[PubMed](#)]
12. Coates, G.W.; Hustad, P.D.; Reinartz, S. Catalysts for the living insertion polymerization of alkenes: Access to new polyolefin architectures using Ziegler–Natta chemistry. *Angew. Chem. Int. Ed.* **2002**, *41*, 2236–2257. [[CrossRef](#)]
13. Xu, G. Copolymerization of ethylene with styrene catalyzed by the $[\eta^1\text{-}\eta^5\text{-tert-butyl}(\text{dimethylfluorenylsilyl})\text{amido}]\text{methyltitanium}$ “Cation”. *Macromolecules* **1998**, *31*, 2395–2402. [[CrossRef](#)]
14. Irwin, L.J.; Reibenspies, J.H.; Miller, S.A. A sterically expanded “constrained geometry catalyst” for highly active olefin polymerization and copolymerization: An unyielding comonomer effect. *J. Am. Chem. Soc.* **2004**, *126*, 16716–16717. [[CrossRef](#)] [[PubMed](#)]
15. Schwerdtfeger, E.D.; Miller, S.A. Intrinsic branching effects in syndiotactic copolymers of propylene and higher α -olefins. *Macromolecules* **2007**, *40*, 5662–5668. [[CrossRef](#)]
16. Schwerdtfeger, E.D.; Price, C.J.; Chai, J.; Miller, S.A. Tandem catalyst system for linear low-density polyethylene with short and long branching. *Macromolecules* **2010**, *43*, 4838–4842. [[CrossRef](#)]
17. Chai, J.; Abboud, K.A.; Miller, S.A. Sterically expanded CGC catalysts: Substituent effects on ethylene and α -olefin polymerization. *Dalton Trans.* **2013**, *42*, 9139–9147. [[CrossRef](#)] [[PubMed](#)]
18. Jung, H.Y.; Hong, S.D.; Jung, M.W.; Lee, H.; Park, Y.W. Norbornene copolymerization with α -olefins using methylene-bridged *ansa*-zirconocene. *Polyhedron* **2005**, *24*, 1269–1273. [[CrossRef](#)]
19. Kirillov, E.; Razaci, A.; Carpentier, J.F. Syndiotactic-enriched propylene–styrene copolymers using fluorenyl-based half-titanocene catalysts. *J. Mol. Catal. A* **2006**, *249*, 230–235. [[CrossRef](#)]
20. Na, S.J.; Wu, C.J.; Yoo, J.; Kim, B.E.; Lee, B.Y. Copolymerization of 5,6-dihydrodicyclopentadiene and ethylene. *Macromolecules* **2008**, *41*, 4055–4057. [[CrossRef](#)]
21. Yu, S.T.; Na, S.J.; Lim, T.S.; Lee, B.Y. Preparation of a bulky cycloolefin/ethylene copolymer and its tensile properties. *Macromolecules* **2010**, *43*, 725–730. [[CrossRef](#)]
22. Nakayama, Y.; Sogo, Y.; Cai, Z.; Shiono, T. Copolymerization of ethylene with 1,1-disubstituted olefins catalyzed by *ansa*-(fluorenyl)(cyclododecylamido)dimethyltitanium complexes. *J. Polym. Sci. Part A* **2013**, *51*, 1223–1229. [[CrossRef](#)]
23. Razavi, A.; Thewalt, U. Preparation and crystal structures of the complexes $(\eta^5\text{-C}_5\text{H}_3\text{TMS-CMe}_2\text{-}\eta^5\text{-C}_{13}\text{H}_8)\text{MCl}_2$ and $[3,6\text{-ditButC}_{13}\text{H}_6\text{-SiMe}_2\text{-NtBu}]\text{MCl}_2$ (M = Hf, Zr or Ti): Mechanistic aspects of the catalytic formation of an isotactic–syndiotactic stereoblock-type polypropylene. *J. Organomet. Chem.* **2001**, *621*, 267–276. [[CrossRef](#)]
24. Busico, V.; Cipullo, R.; Cutillo, F.; Talarico, G.; Razavi, A. Syndiotactic poly(propylene) from $[\text{Me}_2\text{Si}(3,6\text{-di-tert-butyl-9-fluorenyl})(\text{N-tert-butyl})]\text{TiCl}_2$ -based catalysts: Chain-end or enantiotopic-sites stereocontrol? *Macromol. Chem. Phys.* **2003**, *204*, 1269–1274. [[CrossRef](#)]
25. Irwin, L.J.; Miller, S.A. Unprecedented syndioselectivity and syndiotactic polyolefin melting temperature: Polypropylene and poly(4-methyl-1-pentene) from a highly active, sterically expanded η^1 -Fluorenyl- η^1 -amido zirconium complex. *J. Am. Chem. Soc.* **2005**, *127*, 9972–9973. [[CrossRef](#)] [[PubMed](#)]
26. Cai, Z.; Su, H.; Nakayama, Y.; Shiono, T.; Akita, M. Synthesis of C_1 symmetrical *ansa*-cyclopentadienylamidotitanium complexes and their application for living polymerization of propylene. *J. Organomet. Chem.* **2014**, *770*, 136–141. [[CrossRef](#)]

27. Tanaka, R.; Chie, Y.; Cai, Z.; Nakayama, Y.; Shinon, T. Structure-stereospecificity relationships of propylene polymerization using substituted *ansa*-silylene(fluorenyl)(amido) titanium complexes. *J. Organomet. Chem.* **2016**, *804*, 95–100. [[CrossRef](#)]
28. Shiono, T. Living polymerization of olefins with *ansa*-dimethylsilylene(fluorenyl)(amido) dimethyltitanium-based catalysts. *Polym. J.* **2011**, *43*, 331–351. [[CrossRef](#)]
29. Cai, Z.; Su, H.; Shiono, T. Precise synthesis of olefin block copolymers using a syndiospecific living polymerization system. *Chin. J. Polym. Sci.* **2013**, *31*, 541–549. [[CrossRef](#)]
30. Cai, Z.; Ikeda, T.; Akita, M.; Shiono, T. Substituent effects of *tert*-butyl groups on fluorenyl ligand in syndiospecific living polymerization of propylene with *ansa*-fluorenylamidodimethyltitanium complex. *Macromolecules* **2005**, *38*, 8135–8139. [[CrossRef](#)]
31. Shiono, T.; Harada, R.; Cai, Z.; Nakayama, Y. A highly active catalyst composed of *ansa*-fluorenylamidodimethyltitanium derivative for propene polymerization. *Top. Catal.* **2009**, *52*, 675–680. [[CrossRef](#)]
32. Cai, Z.; Nakayama, Y.; Shiono, T. Substituent effects of *tert*-butyl groups on fluorenyl ligand of [t-BuNSiMe₂Flu]ZrMe₂. *Chin. J. Polym. Sci.* **2008**, *31*, 575–578. [[CrossRef](#)]
33. Sun, Y.; Xu, B.; Shiono, T.; Cai, Z. Highly active *ansa*-(Fluorenyl)(amido)titanium-based catalysts with low load of methylaluminoxane for syndiotactic-specific living polymerization of propylene. *Organometallics* **2017**, *36*, 3009–3012. [[CrossRef](#)]
34. Song, X.; Ma, Q.; Yuan, H.; Cai, Z. Synthesis of hydroxy-functionalized ultrahigh molecular weight polyethylene using fluorenylamidotitanium complex. *Chin. J. Polym. Sci.* **2017**. [[CrossRef](#)]
35. Sheldrick, G.M. *SADABS: An Empirical Absorption Correction Program for Area Detector Data*; University of Göttingen: Göttingen, Germany, 1996.
36. Sheldrick, G.M. Crystal structure refinement with SHELXL. *Acta Crystallogr. Sect. C* **2015**, *C71*, 3–8.
37. Sheldrick, G.M. A short history of SHELX. *Acta Crystallogr. Sect. A* **2008**, *A64*, 112–122. [[CrossRef](#)] [[PubMed](#)]
38. Dolomanov, O.V.; Bourhis, L.J.; Gildea, R.J.; Howard, J.A.; Puschmann, H. OLEX2: A complete structure solution, refinement and analysis program. *J. Appl. Crystallogr.* **2009**, *42*, 339–341. [[CrossRef](#)]
39. SAINT+, version 6.22a; Bruker AXS Inc.: Madison, WI, USA, 2002.
40. SAINT+, version v7.68A; Bruker AXS Inc.: Madison, WI, USA, 2009.
41. SHELXTL NT/2000, version 6.1; Bruker AXS Inc.: Madison, WI, USA, 2002.
42. Tolman, C.A. Formation of three-coordinate nickel(0) complexes by phosphorus ligand dissociation from NiL₄. *J. Am. Chem. Soc.* **1974**, *96*, 53–60. [[CrossRef](#)]
43. Hansch, C.; Leo, A.; Taft, R.W. A survey of Hammett substituent constants and resonance and field parameters. *Chem. Rev.* **1991**, *91*, 165–195. [[CrossRef](#)]
44. Busico, V.; Cipullo, R.; Cuttillo, F.; Friederichs, N.; Ronca, S.; Wang, B. Improving the performance of methylalumoxane: A facile and efficient method to trap “free” trimethylaluminum. *J. Am. Chem. Soc.* **2003**, *125*, 12402–12403. [[CrossRef](#)] [[PubMed](#)]
45. Cipullo, R.; Busico, V.; Fraldi, N.; Pellecchia, R.; Talarico, G. Improving the behavior of bis(phenoxyamine) Group 4 metal catalysts for controlled alkene polymerization. *Macromolecules* **2009**, *42*, 3869–3872. [[CrossRef](#)]
46. Cai, Z.; Nakayama, Y.; Shiono, T. Facile synthesis of tailor-made stereoblock polypropylenes via successive variation of monomer pressure. *Macromolecules* **2008**, *41*, 6596–6598. [[CrossRef](#)]

